⌘ *Author's Choice*

THE JOURNAL OF BIOLOGICAL CHEMISTRY VOL. 286, NO. 43, pp. 37274–37279, October 28, 2011

MYPT1 Protein Isoforms Are Differentially Phosphorylated by Protein Kinase G*[S]

Received for publication, July 15, 2011, and in revised form, August 11, 2011 Published, JBC Papers in Press, September 2, 2011, DOI 10.1074/jbc.M111.282905

Samantha Yuen, Ozgur Ogut, and Frank V. Brozovich[1]

From the Department of Cardiovascular Diseases, Mayo Medical School, Rochester, Minnesota 55905

Background: The mechanism by which PKGIα activates MLC phosphatase with an LZ+ (but not LZ−) MYPT1 isoform is unknown.
Results: LZ+ MYPT1 fragments are rapidly phosphorylated by PKGIα at Ser-667 and Ser-694.
Conclusion: MYPT1 isoform expression is important for determining the response of vascular beds to NO and NO-based vasodilators.
Significance: MYPT1 isoform expression plays a central role in the regulation of vascular tone in health and disease.

Smooth muscle relaxation in response to NO signaling is due, in part, to a Ca^{2+}-independent activation of myosin light chain (MLC) phosphatase by protein kinase G Iα (PKGIα). MLC phosphatase is a trimeric complex of a 20-kDa subunit, a 38-kDa catalytic subunit, and a 110–133-kDa myosin-targeting subunit (MYPT1). Alternative mRNA splicing produces four MYPT1 isoforms, differing by the presence or absence of a central insert and leucine zipper (LZ). The LZ domain of MYPT1 has been shown to be important for PKGIα-mediated activation of MLC phosphatase activity, and changes in LZ+ MYPT1 isoform expression result in changes in the sensitivity of smooth muscle to NO-mediated relaxation. Furthermore, PKGIα has been demonstrated to phosphorylate Ser-694 of MYPT1, but phosphorylation at this site does not always accompany cGMP-mediated smooth muscle relaxation. This study was designed to determine whether MYPT1 isoforms are differentially phosphorylated by PKGIα. The results demonstrate that purified LZ+ MYPT1 fragments are rapidly phosphorylated by PKGIα at Ser-667 and Ser-694, whereas fragments lacking the LZ domain are poor PKGIα substrates. Mutation of Ser-667 and Ser-694 to Ala and/or Asp showed that Ser-667 phosphorylation is more rapid than Ser-694 phosphorylation, suggesting that Ser-667 may play an important role in the activation of MLC phosphatase. These results demonstrate that MYPT1 isoform expression is important for determining the heterogeneous response of vascular beds to NO and NO-based vasodilators, thereby playing a central role in the regulation of vascular tone in health and disease.

Activation of smooth muscle is dependent on the level of phosphorylation of the 20-kDa regulatory smooth muscle myosin light chain (MLC),[2] which is determined by the relative activities of MLC kinase and MLC phosphatase (1, 2). MLC kinase is regulated by Ca^{2+} (3), whereas a number of signaling pathways regulate the activity of MLC phosphatase (4, 5), a trimeric complex consisting of a small 20-kDa subunit, a 38-kDa catalytic subunit, and a myosin-targeting subunit (MYPT1) of 110–133 kDa (4). Alternative mRNA splicing produces four MYPT1 isoforms (4), which differ by the presence or absence of a central insert (CI) and a C-terminal leucine zipper (LZ). Isoform expression is both developmentally regulated and tissue-specific (6, 7).

Smooth muscle relaxation in response to NO is a fundamental response of the vasculature (8); in the vasculature, an increase in flow increases shear stress on endothelial cells, which stimulates NO production. NO diffuses into the smooth muscle cells to activate the soluble pool of guanylate cyclase to increase the intracellular concentration of cGMP. cGMP can bind and activate protein kinase G, which subsequently acts on a number of targets to decrease intracellular Ca^{2+} (9–11) and also leads to a Ca^{2+}-independent activation of MLC phosphatase (12). There is ample experimental evidence that the LZ domain of MYPT1 is required for protein kinase G Iα (PKGIα)-mediated activation of MLC phosphatase (12–14), and changes in LZ+ MYPT1 isoform expression result in changes in the sensitivity of smooth muscle to NO-mediated relaxation in health and disease (7, 14–19).

The mechanism for PKGIα-mediated activation of MLC phosphatase activity is unknown. Using a recombinant MYPT1 fragment (MYPT1CI−LZ+), Haystead and co-workers (20) identified three MYPT1 phosphorylation sites (Ser-692, Ser-695, and Ser-852 of the mammalian sequence; equivalent to Ser-691, Ser-694, and Ser-849 of the avian sequence), and PKGIα-mediated MYPT1 phosphorylation at Ser-695 resulted in the exclusion of Rho kinase-mediated MYPT1 phosphorylation at Thr-696. These results were confirmed by Ikebe and co-workers (21), who also demonstrated that Ser-695 phosphorylation did not change MLC phosphatase activity but prevented the decrease in MLC phosphatase activity produced by Rho kinase phosphorylation at Thr-696. However, others have demonstrated that increases in Ser-695 phosphorylation are not observed during cGMP-mediated relaxation of cerebral vessels (22).

* This work was supported by the Mayo Clinic.
[S] The on-line version of this article (available at http://www.jbc.org) contains supplemental Fig. 1.
⌘ *Author's Choice*—Final version full access.
[1] To whom correspondence should be addressed: Dept. of Cardiovascular Diseases, Mayo Medical School, 200 1st St. SW, Rochester, MN 55905. Tel.: 507-266-0324; Fax: 507-238-6418; E-mail: brozovich.frank@mayo.edu.
[2] The abbreviations used are: MLC, myosin light chain; CI, central insert; LZ, leucine zipper; PKGIα, protein kinase G Iα.

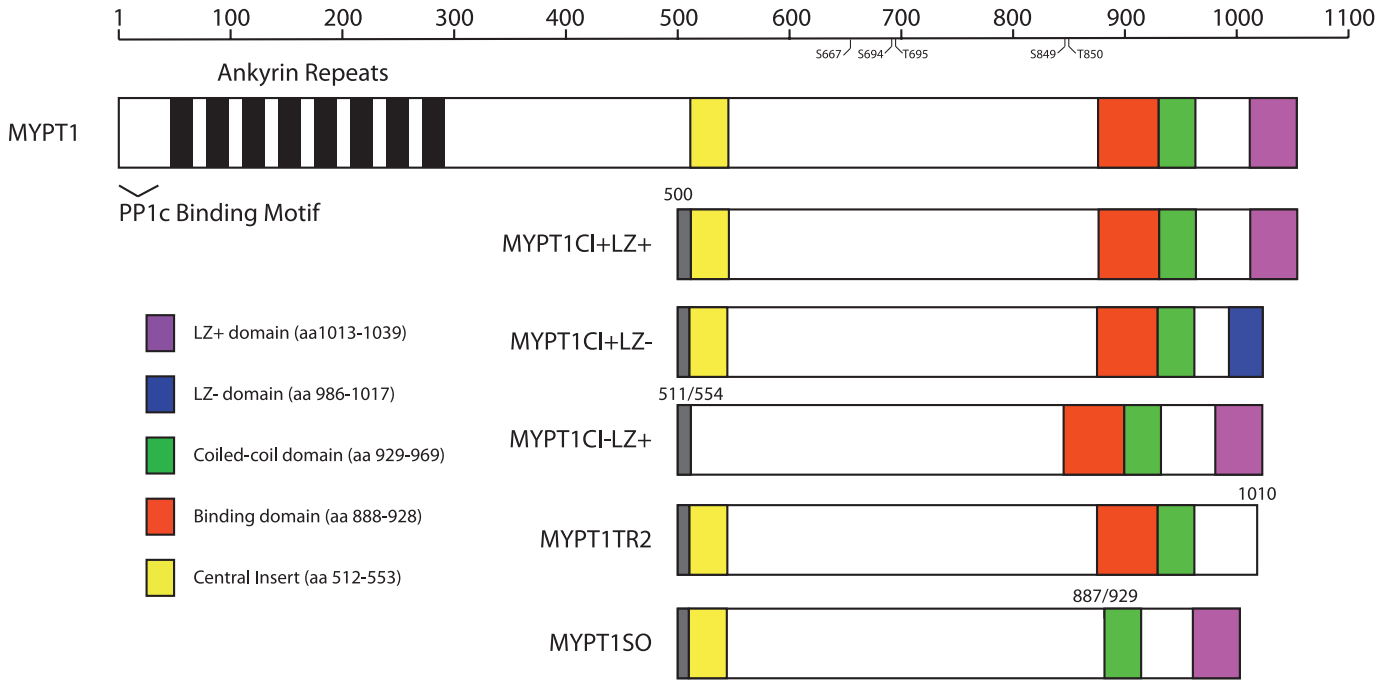

FIGURE 1. **MYPT1 fragments.** Shown are the structures of the endogenous chicken MYPT1CI+LZ+ isoform and MYPT1 fragment proteins. Phosphorylation sites are also indicated (avian sequence).

Given the diversity in MYPT1 isoform expression among vascular beds (6, 7), these results could suggest that MYPT1 structure influences PKGIα phosphorylation, and/or MYPT1 isoforms are differentially phosphorylated by PKGIα. Differential MYPT1 phosphorylation could explain the heterogeneous response to NO-mediated vasodilatation among vascular beds that have unique MYPT1 isoform expression patterns. To test this hypothesis, we determined the effect of the structure of MYPT1 on the rate and extent of its phosphorylation by PKGIα.

EXPERIMENTAL PROCEDURES

Cloning of MYPT1 Mutants—Four mutant MYPT1 plasmids were created from an avian MYPT1CI−LZ+ template (23) using the QuikChange site-directed mutagenesis Kit (Stratagene). Mutagenesis primers were generated to mutate Ser-667 or Ser-694 (equivalent to Ser-668 and Ser-695 of the mammalian sequence) to either Ala to prevent phosphorylation or Asp to mimic phosphorylation, yielding the following MYPT1 mutants: S667A, S667D, S694A, and S694D. All mutants were sequenced to confirm the desired mutation, and unless noted otherwise, we refer to the avian sequence throughout this work (Fig. 1).

Protein Expression and Purification—Plasmids expressing all MYPT1 variants were transformed into BL21 Star *E. coli* competent cells (Invitrogen) and purified without purification tags as described previously (23). Briefly, nutrient-rich medium containing 100 μg/ml ampicillin and 25 μg/ml chloramphenicol was inoculated with freshly plated bacteria and grown to $A_{600\,nm}$ = 0.4–0.6, at which time, protein expression was induced with 0.2 mM isopropyl β-D-1-thiogalactopyranoside. Protein expression was allowed to continue for 3 h before the bacteria were collected, and pellets were stored at −80 °C overnight. After thawing, cells were resuspended in buffer containing 20 mM diethanolamine (pH 8.7), 0.1 mM EDTA, 10 mM β-mercaptoethanol, and 1× Complete protease inhibitor (Roche Applied Science) prior to sonication. Once the cells were lysed, 10 units of DNase I (Roche Applied Science) were added to the mixture and left to rotate at 4 °C for 45 min before centrifugation. The resulting supernatant was subjected to ammonium sulfate extractions to 35 and 65% saturation. The 35% pellet containing the desired MYPT1 protein was dialyzed overnight against 4 liters of 20 mM MES (pH 6.0), 0.1 mM EDTA, and 10 mM β-mercaptoethanol. To increase the protein solubility of the dialyzed sample, urea was dissolved to a final concentration of 6 M. Following dialysis, the sample was then centrifuged and syringe-filtered before undergoing cation exchange chromatography using a similarly equilibrated SOURCE 15S column (GE Healthcare). The desired fractions (eluted with a 0.5 M NaCl linear gradient) were subsequently buffer-exchanged into 6 M urea, 30 mM diethanolamine (pH 8.5), 0.1 mM EDTA, and 10 mM β-mercaptoethanol by gel filtration and then resolved by Mono Q chromatography and developed with a linear gradient to 0.5 M NaCl. Fractions containing MYPT1 were dialyzed against 50 mM ammonium bicarbonate and lyophilized.

MYPT1 Phosphorylation—The lyophilized MYPT1 variants were each dissolved in storage buffer containing 300 mM NaCl, 2 mM HEPES (pH 7.0), and 1 mM β-mercaptoethanol and tested individually. Per reaction, 0.1 nmol of MYPT1 was added to reaction buffer containing 1 mM ATP, 0.1 mM cGMP, 100 mM NaCl, 10 mM HEPES (pH 7.0), 0.1 mM $MgCl_2$, and 10 mM β-mercaptoethanol. PKGIα (48 units; Promega) was added, and aliquots from the reaction were drawn at 1, 5, 10, 20, and 60 min along with a corresponding untreated MYPT1 sample to

serve as a control. Reactions were carried out at room temperature, stopped with 4× lithium dodecyl sulfate buffer, and resolved by 10% SDS-PAGE (29:1). MYPT1 phosphorylation was determined using Pro-Q® Diamond stain (Invitrogen), and total protein was subsequently determined on the same gel using either Deep Purple™ total protein stain (GE Healthcare) or colloidal Coomassie Blue. Bands were quantified using ImageQuant TL software, and phosphorylation rates were calculated by fitting the data of phosphorylation/total protein *versus* time with a single exponential.

For Rho kinase-mediated phosphorylation, the MYPT1 fragments were phosphorylated using our previously published protocol (24). Briefly, 0.1 nmol of the purified MYPT1 fragment was incubated with 0.1 μg/ml Rho kinase (Upstate Biotechnology) at 25 °C in assay buffer containing 100 mM NaCl, 0.1 mM $MgCl_2$, 0.1 mM cGMP, 1.0 mM ATP, and 10 mM HEPES (pH 7) for 60 min. The reaction was stopped with lithium dodecyl sulfate buffer. Samples were then resolved by SDS-PAGE, and phosphorylation sites were identified by immunoblotting with phospho-specific antibodies.

Immunoblotting—Immunoblotting was performed as described previously (23). During the purification processes, MYPT1 variants were identified using either an anti-MYPT1 monoclonal antibody (1C2) or an anti-MYPT1 polyclonal antibody (Upstate Biotechnology). MYPT1 phosphorylation was also determined using phospho-specific anti-Ser-695 and anti-Ser-852/Thr-853 antibodies (generously provided by Dr. Mitsuo Ikebe). Phosphorylation at Thr-696 and Thr-853 was assessed using phospho-specific anti-Thr-696 and anti-Thr-853 antibodies (Santa Cruz Biotechnology).

Mass Spectrometry—To characterize PKGIα-mediated MYPT1 phosphorylation, we used electron transfer dissociation technology on an LTQ Orbitrap mass spectrometer (Mayo Proteomics Research Core). Electron transfer dissociation enables peptide dissociation by transferring electrons from a negatively charged molecule to positively charged peptides. The energetic transfer results in a ladder of *c* and *z* ions with post-translational modifications left intact. Thus, not only the presence but also the location of phosphorylation and other post-translational modifications can be easily located. Phosphopeptides can be easily enriched from any Lys-C digest by passing the digest over an immobilized metal affinity column. These enriched peptides are then separated by reversed-phase nano-HPLC directly into the LTQ Orbitrap ion source. Lys-C is utilized to yield peptides with higher charge states than is usually obtained by a trypsin digest. Higher charge state peptides are more amenable to electron transfer dissociation fragmentation. The resulting data are searched, allowing for phosphorylation as a variable modification in database searches (25).

Data Analysis—All data are expressed as the mean ± S.E., and Student's *t* test was used to compare means, with $p < 0.05$ chosen for significance.

RESULTS

We have demonstrated previously that sequence 888–928 is important for the interaction of our MYPT1 fragments with PKGIα (23), which has since been confirmed by other investigators (26). Furthermore, our MYPT1 fragments compete with endogenous MYPT1 for the interaction with PKGIα (23), and immunoblotting with phospho-specific anti-MYPT1 antibodies (Fig. 2) demonstrated that the MYPT1 fragments were phosphorylated at Ser-694 (Ser-695 of the mammalian sequence) by PKGIα and at Thr-695 and Thr-850 (Thr-696 and Thr-853 of the mammalian sequence) by Rho kinase. These data suggest that the structures of the MYPT1 fragments are similar to that of the intact protein and preserve the specificity of kinase-mediated phosphorylation.

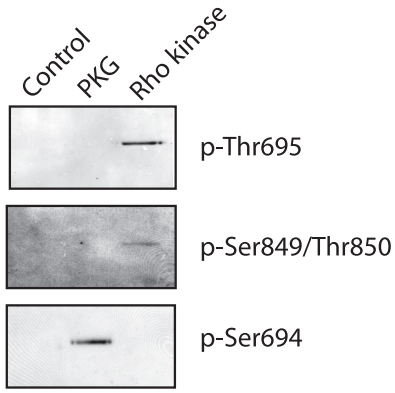

FIGURE 2. **Phosphorylation of MYPT1 fragments by Rho kinase and PKGIα.** The MYPT1 fragments were phosphorylated by PKGIα or Rho kinase. *First lane*, control without PKGIα or Rho kinase; *second lane*, PKGIα treatment; *third lane*, treatment with Rho kinase. The anti-Ser-694 antibody (Ser-695 of the mammalian sequence) reacted with MYPT1 treated with PKGIα, but phosphorylation was not detected at Ser-849 (Ser-852 of the mammalian sequence). For Rho kinase, MYPT1 was phosphorylated at both Thr-695 and Thr-850 (Thr-696 and Thr-853 of the mammalian sequence).

To examine whether the presence or absence of the MYPT1 LZ domain influences PKGIα-mediated MYPT1 phosphorylation, the rate and extent of phosphorylation of the MYPT1 fragments representing endogenous MYPT1CI+LZ+ and MYPT1CI+LZ− were determined (Fig. 3). Activation of PKGIα resulted in a rapid increase in the phosphorylation of MYPT1CI+LZ+; the rate of PKGIα-mediated phosphorylation was 0.31 ± 0.07 min^{-1} (Fig. 3). This contrasts with the results for the LZ− fragment (MYPT1CI+LZ−), wherein PKGIα treatment did not produce detectable phosphorylation of the LZ− fragment (Fig. 3). The role of the CI was examined by determining the rate and extent of PKGIα-mediated phosphorylation of MYPT1CI−LZ+; the CI did not influence the extent of phosphorylation, but the rate of PKGIα-mediated phosphorylation was significantly lower (0.08 ± 0.03 min^{-1}) than that observed for the MYPT1CI+LZ+ fragment.

We next investigated the ability of other MYPT1 domains to modulate PKGIα-mediated phosphorylation by comparing the rate and extent of phosphorylation of our previously characterized MYPT1 fragments (Fig. 1) (23). MYPT1SO contains the CI and LZ domain but lacks the PKGIα-binding domain at amino acids 888–928, whereas MYPT1TR2 contains both the CI and PKGIα-binding domains but is truncated at the C terminus and lacks the LZ domain. MYPT1SO was phosphorylated by PKGIα, but the rate and extent were lower than those of MYPT1CI+LZ+ (Fig. 4). Similar to MYPT1CI+LZ−, MYPT1TR2 was a poor substrate for PKGIα (Fig. 4), indicating the importance of the LZ domain of MYPT1 for PKGIα-mediated phosphorylation.

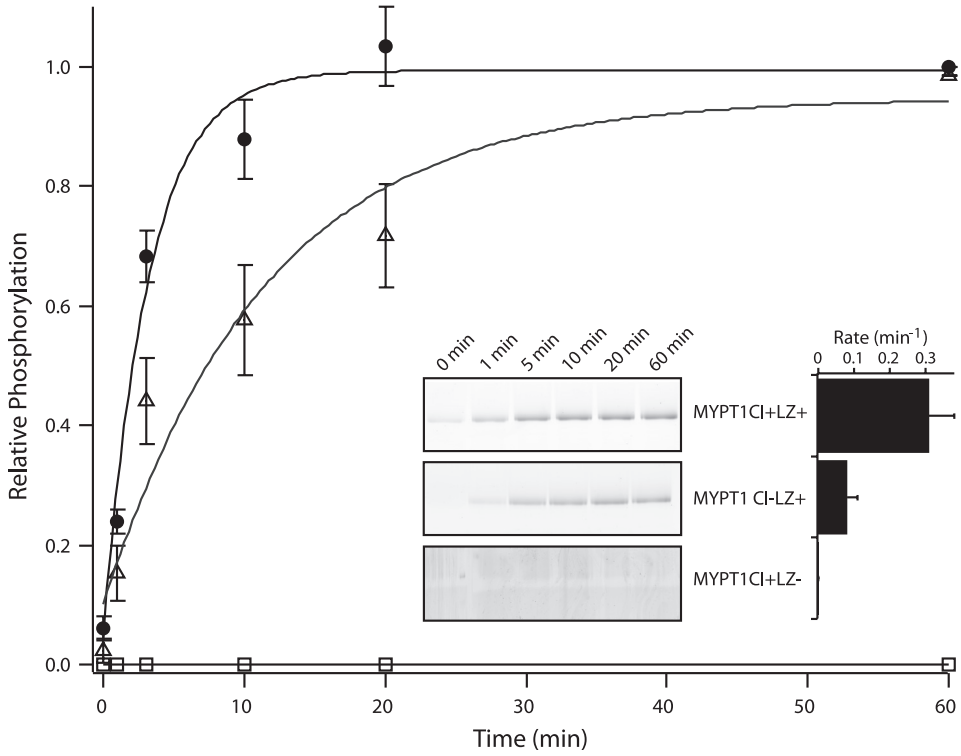

FIGURE 3. **PKGIα phosphorylation of protein fragments representing the endogenous MYPT1 isoforms.** The time course of MYPT1 phosphorylation by PKGIα was determined by dividing the intensity of the band on the Pro-Q Diamond phosphoprotein-stained gel by the total protein (intensity of the MYPT1 band following subsequent Deep Purple staining of the same gel), and the data were fit to a single exponential equation. The rate and extent of MYPT1CI+LZ+ (0.31 ± 0.07 min^{-1}; ●) and MYPT1CI−LZ+ (0.08 ± 0.03 min^{-1}; △) phosphorylation were significantly higher than those of MYPT1CI+LZ− (□), which was not significantly phosphorylated by PKGIα. *Inset*, Pro-Q Diamond phosphoprotein-stained gels of MYPT1CI+LZ+, MYPT1CI−LZ+, and MYPT1CI+LZ− demonstrate phosphorylation of MYPT1 fragments at equal protein loading, and the bar graph summarizes rates of phosphorylation.

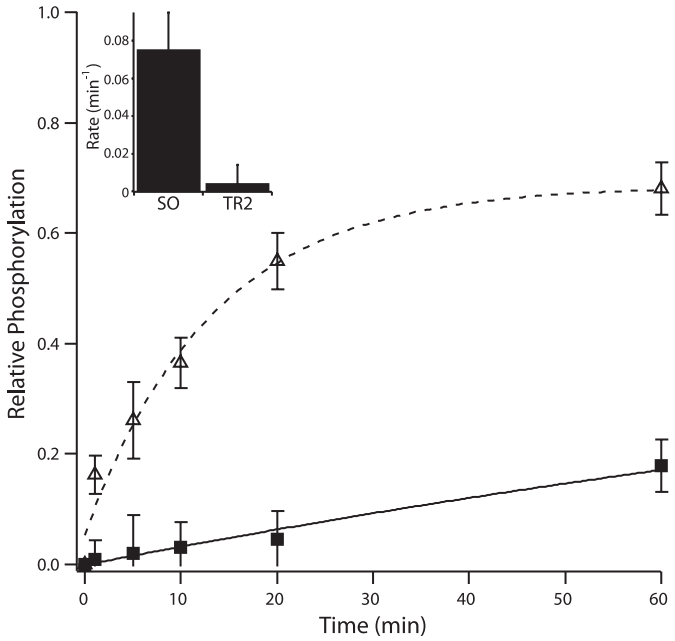

FIGURE 4. **PKGIα phosphorylation of MYPT1SO and MYPT1TR2.** The time course of MYPT1 phosphorylation by PKGIα was determined by dividing the intensity of the band on the Pro-Q Diamond phosphoprotein-stained gel by the total protein (intensity of the MYPT1 band following subsequent Deep Purple staining of the same gel), and the data were fit to a single exponential equation. MYPT1SO (△) was phosphorylated by PKGIα (0.075 ± 0.02 min^{-1}), but MYPT1TR2 (■), which lacks the LZ domain, was a poor substrate for PKGIα (0.004 ± 0.01 min^{-1}; $p < 0.05$). Data for relative phosphorylation were normalized to a maximum of 1 (MYPT1CI+LZ+). *Inset*, bar graph summarizing rates of phosphorylation.

For MYPT1CI+LZ+, mass spectrometry identified the phosphopeptides pSTQGVTLTDLQEAEK, RRpSYLTPVR, and pSYLTPVRDEESESQR (supplemental Fig. 1), which are consistent with PKGIα-mediated phosphorylation of MYPT1CI+LZ+ at Ser-667 and Ser-694 of the avian sequence (Ser-668 and Ser-695 of the mammalian sequence). Similar phosphopeptide sequences were obtained for all MYPT1 fragments and mutants, indicating that PKGIα phosphorylates all MYPT1 isoforms at Ser-667 and Ser-694.

We next examined PKGIα-mediated phosphorylation of the MYPT1 mutants S667A, S667D, S694A, and S694D (Fig. 5). For the S667A and S667D mutants, the rates of phosphorylation were similar (0.017 ± 0.001 *versus* 0.024 ± 0.004 min^{-1}). PKGIα-mediated phosphorylation of the S694A and S694D mutants was more rapid than that of the S667A and S667D mutants; the rate of PKGIα-mediated phosphorylation of S694A was 0.060 ± 0.002 min^{-1}, which increased significantly when this residue was mutated to Asp (S694D; 0.13 ± 0.02 min^{-1}).

DISCUSSION

We have demonstrated previously that changes in LZ+/LZ− MYPT1 expression cause changes in the sensitivity of cGMP-mediated smooth muscle relaxation (14), and there is diversity in LZ+/LZ− MYPT1 isoform expression and cGMP-mediated smooth muscle relaxation among vascular beds in normal animals (7, 14). Furthermore, decreases in LZ+ isoform expression and cGMP-mediated smooth muscle relaxation have been

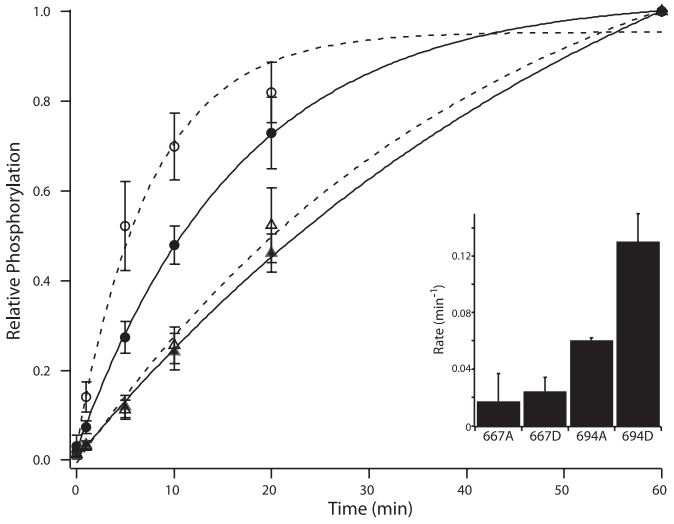

FIGURE 5. **PKGIα phosphorylation of MYPT1 mutants.** The time course of MYPT1 phosphorylation by PKGIα was determined by dividing the intensity of the band on the Pro-Q Diamond phosphoprotein-stained gel by the total protein (intensity of the MYPT1 band following subsequent Deep Purple staining of the same gel), and the data were fit to a single exponential equation. The rates of phosphorylation of MYPT1 S667A (*667A*; 0.017 ± 0.001 min^{-1}; ▲) and S667D (*667D*; 0.024 ± 0.004 min^{-1}; △) were similar. However, the rates of phosphorylation of the S694A (*694A*) and S694D (*694D*) mutants were significantly higher. For S694A (●), the rate of phosphorylation was 0.060 ± 0.002 min^{-1}, and the rate was significantly higher for S694D (0.13 ± 0.02 min^{-1}; ○). *Inset*, bar graph summarizing rates of phosphorylation.

demonstrated in animal models of disease (15–19). In addition, we have shown previously that our MYPT1 fragments compete with endogenous MYPT1 for PKGIα binding, and data from this study demonstrate that the MYPT1 fragments are phosphorylated at previously characterized *in vivo* phosphorylation sites (Fig. 2). Therefore, these data suggest that the MYPT1 fragments are suitable for studies designed to examine the phosphorylation mechanism.

Our results demonstrate that MYPT1 structure is important for PKGIα-mediated phosphorylation of the protein. LZ+ MYPT1 fragments (MYPT1CI+LZ+, MYPT1CI−LZ+, and MYPT1SO) were phosphorylated by PKGIα, whereas MYPT1 fragments lacking the LZ domain (MYPT1CI+LZ− and MYPT1TR2) were poor substrates (Figs. 3 and 4). MYPT1TR2 is similar to the MYPT1CI+LZ+ fragment but lacks the LZ domain (Fig. 1). Its rate (0.004 min^{-1}) and extent of phosphorylation by PKGIα were significantly less than those of any LZ+ MYPT1 fragment tested, indicating the importance of the LZ domain for PKGIα phosphorylation. These data also suggest that the structures of LZ+ and LZ− MYPT1 isoforms are different; PKG phosphorylation sites may be exposed in LZ+ MYPT1 isoforms but not in LZ− MYPT1 isoforms. Alternatively, the interaction of LZ+ (but not LZ−) MYPT1 isoforms with PKGIα increased the kinase activity, resulting in differential phosphorylation. The presence or absence of the CI also modulated PKGIα-mediated MYPT1 phosphorylation; although total phosphorylation was similar, the rate of phosphorylation of MYPT1CI+LZ+ was significantly higher than that of MYPT1CI−LZ+ (Fig. 3). Thus, these data suggest that MYPT1 structure is important for PKGIα-mediated phosphorylation, and structural differences contribute to differential phosphorylation of the endogenous MYPT1 isoforms by controlling the extent and rate of phosphorylation.

The interaction of PKGIα with MYPT1 may occur through multiple sites. Our previous studies have shown that there is a major PKGIα-binding domain between amino acids 888 and 928 of MYPT1, as judged by the MYPT1SO fragment, which lacks this motif and does not bind PKGIα (23). Others have demonstrated that the LZ domain of MYPT1 also mediates the interaction with PKGIα (26, 27). The results in Fig. 4 suggest that the absence of sequence 888–928 likely results in an impairment of the PKGIα and MYPT1SO interaction so as to decrease, but not abolish, phosphorylation. However, it is clear that the LZ domain is required for efficient PKGIα-mediated MYPT1 phosphorylation. Comparison of the PKGIα-mediated phosphorylation of the fragments representing the endogenous LZ+ (MYPT1CI+LZ+ and MYPT1CI−LZ+) and LZ− (MYPT1CI+LZ−) MYPT1 isoforms revealed that the LZ+ fragments were rapidly phosphorylated by PKGIα, whereas phosphorylation was not detected in the LZ− fragment. The results with MYPT1TR2 are consistent with these findings; MYPT1TR2 is the MYPT1CI+LZ+ fragment lacking only the LZ domain (Fig. 1), rendering it a poor substrate for PKGIα (Fig. 4).

Haystead and co-workers (20) have demonstrated that MYPT1 is phosphorylated at Ser-692, Ser-695, and Ser-852 of the mammalian sequence by PKGIα. Both Haystead and co-workers (20) and Ikebe and co-workers (21) have demonstrated that Ser-695 phosphorylation does not change phosphatase activity, but rather the resulting exclusion of Rho kinase-mediated phosphorylation at Thr-696 prevents a Rho kinase-mediated decrease in MLC phosphatase activity. Haystead and co-workers suggested that PKGIα-mediated phosphorylation at Ser-852 also excludes Rho kinase-mediated phosphorylation at Thr-853 but did not comment on the effect of Ser-692 phosphorylation. Using mass spectrometry, we have mapped PKGIα phosphorylation to Ser-667 and Ser-694 of the avian sequence, and these phosphorylation sites were identified in every MYPT1 fragment tested. However, in the study by Haystead and co-workers (20), the phosphorylation was mapped using an MYPT1CI−LZ+ fragment, and it is possible that phosphorylation at sites other than Ser-667 and Ser-694 (equivalent to Ser-668 and Ser-695 of the mammalian sequence) could vary among the four MYPT1 isoforms. Nonetheless, our results provide an explanation for the lack of Ser-694 phosphorylation observed by Somlyo and co-workers during cGMP-mediated relaxation of cerebral arteries (22); cerebral arteries express the LZ+ MYPT1 isoforms, but expression appears much lower compared with the LZ− MYPT1 isoforms, which suggests that changes in Ser-695 phosphorylation may be difficult to detect.

The rates of phosphorylation for the avian MYPT1 S667A and S667D mutants were similar, although both were slower compared with the Ser-694 mutants (Fig. 5). PKGIα-mediated phosphorylation of S694A was faster than that of S667A and S667D, and changing Ser-694 to a phospho-mimicking residue (S694D) further enhanced the rate of MYPT1 phosphorylation (Fig. 5). Presumably, the S667A and S667D mutants are phosphorylated predominantly at Ser-694, whereas the S694A and S694D mutants are phosphorylated at Ser-667. These results

suggest that phosphorylation of Ser-694 (Ser-695 of the mammalian sequence) is slower than that of Ser-667 (S668 of the mammalian sequence), and pre-phosphorylation of MYPT1 at Ser-694 enhances the subsequent rate of phosphorylation at Ser-667. Taken together, the results would be consistent with MYPT1 phosphorylation at Ser-667 preceding phosphorylation at Ser-694 during NO-mediated smooth muscle relaxation. NO-mediated smooth muscle relaxation is rapid, and these data suggest that the physiologically important MYPT1 phosphorylation occurs at a site that is rapidly phosphorylated by PKGIα (Ser-667).

There are a number of mechanisms that produce smooth muscle relaxation in response to NO-cGMP-PKG signaling. These include Ca^{2+}-dependent mechanisms (9–11), a Ca^{2+}-independent activation of MLC phosphatase (13, 14), and signaling involving telokin (28, 29). The Ca^{2+}-independent processes are referred to as Ca^{2+} desensitization because smooth muscle relaxation occurs without a change in intracellular Ca^{2+} (30). The major pathway for Ca^{2+} desensitization is a PKGIα-induced increase in MLC phosphatase activity and a resulting decrease in smooth muscle MLC phosphorylation and force (5). However, there is diversity in sensitivity of smooth muscle to NO-mediated relaxation (7, 14–19), and our results suggest that the mechanism for the heterologous response of smooth muscle to NO- and nitrate-based vasodilators lies, in part, at the level of the smooth muscle. Smooth muscles that express predominantly LZ+ MYPT1 isoforms are rapidly phosphorylated by PKGIα and are sensitive to Ca^{2+} desensitization, whereas LZ− MYPT1 isoforms are poor PKGIα substrates and are not sensitive to Ca^{2+} desensitization. On the other hand, smooth muscles that express predominantly LZ− MYPT1 isoforms and/or PKGIβ, which does not interact with MYPT1 (7), may rely on Ca^{2+}-dependent mechanisms (9–11) to relax in response to NO. Furthermore, the CI also modulates PKGIα-mediated phosphorylation, and there are multiple PKGIα phosphorylation sites, which would allow for an additional level for fine-tuning the vascular response to NO.

The roles of Ser-667 and/or Ser-694 phosphorylation during NO-mediated smooth muscle relaxation will require further study. However, our results demonstrate that MYPT1 structure affects PKGIα-mediated phosphorylation and provide a molecular mechanism to explain the differences in cGMP-mediated Ca^{2+} desensitization of LZ+/LZ− MYPT1 isoforms; LZ+ MYPT1 isoforms are rapidly phosphorylated by PKGIα, whereas LZ− MYPT1 isoforms are poor PKGIα substrates. In addition, although the LZ domain is required for PKGIα-mediated phosphorylation, the CI also modulates the rate of phosphorylation. These results provide a molecular mechanism to explain the diversity in the response of various vascular beds to NO-mediated vasodilatation. Furthermore, the expression of both the CI (6) and LZ domain (7) is developmentally regulated, and the expression of LZ+ MYPT1 isoforms decreases in animal models of heart failure (15, 19), preeclampsia (18), and portal hypertension (16). This decrease in the relative expression of LZ+ MYPT1 isoforms would explain the decrease in sensitivity to NO-mediated vasodilatation and contribute to the increase in vascular tone observed in these diseases. Taken together, these results suggest that MYPT1 isoform expression is important for the regulation of vascular tone and reactivity in health and disease.

REFERENCES

1. Gong, M. C., Cohen, P., Kitazawa, T., Ikebe, M., Masuo, M., Somlyo, A. P., and Somlyo, A. V. (1992) *J. Biol. Chem.* **267,** 14662–14668
2. Ogut, O., and Brozovich, F. V. (2000) *Am. J. Physiol. Cell Physiol.* **279,** C1722–C1732
3. Hartshorne, D. J. (1987) *Physiology of the Gastrointestinal Tract*, Raven Press, New York
4. Hartshorne, D. J., Ito, M., and Erdödi, F. (1998) *J. Muscle Res. Cell Motil.* **19,** 325–341
5. Somlyo, A. P., and Somlyo, A. V. (2003) *Physiol. Rev.* **83,** 1325–1358
6. Dirksen, W. P., Vladic, F., and Fisher, S. A. (2000) *Am. J. Physiol. Cell Physiol.* **278,** C589–C600
7. Khatri, J. J., Joyce, K. M., Brozovich, F. V., and Fisher, S. A. (2001) *J. Biol. Chem.* **276,** 37250–37257
8. Furchgott, R. F. (1999) *Biosci. Rep.* **19,** 235–251
9. Alioua, A., Tanaka, Y., Wallner, M., Hofmann, F., Ruth, P., Meera, P., and Toro, L. (1998) *J. Biol. Chem.* **273,** 32950–32956
10. Schmidt, H. H., Lohmann, S. M., and Walter, U. (1993) *Biochim. Biophys. Acta* **1178,** 153–175
11. Fukao, M., Mason, H. S., Britton, F. C., Kenyon, J. L., Horowitz, B., and Keef, K. D. (1999) *Pflugers Arch.* **274,** 10927–10935
12. Surks, H. K., and Mendelsohn, M. E. (2003) *Cell. Signal.* **15,** 937–944
13. Surks, H. K., Mochizuki, N., Kasai, Y., Georgescu, S. P., Tang, K. M., Ito, M., Lincoln, T. M., and Mendelsohn, M. E. (1999) *Science* **286,** 1583–1587
14. Huang, Q. Q., Fisher, S. A., and Brozovich, F. V. (2004) *J. Biol. Chem.* **279,** 597–603
15. Chen, F. C., Ogut, O., Rhee, A. Y., Hoit, B. D., and Brozovich, F. V. (2006) *J. Mol. Cell. Cardiol.* **41,** 488–495
16. Zhang, H., and Fisher, S. A. (2007) *Circ. Res.* **100,** 730–737
17. Payne, M. C., Zhang, H. Y., Shirasawa, Y., Koga, Y., Ikebe, M., Benoit, J. N., and Fisher, S. A. (2004) *Am. J. Physiol. Heart Circ. Physiol.* **286,** H1801–H1810
18. Lu, Y., Zhang, H., Gokina, N., Mandala, M., Sato, O., Ikebe, M., Osol, G., and Fisher, S. A. (2008) *Am. J. Physiol. Cell Physiol.* **294,** C564–C571
19. Karim, S. M., Rhee, A. Y., Given, A. M., Faulx, M. D., Hoit, B. D., and Brozovich, F. V. (2004) *Circ. Res.* **95,** 612–618
20. Wooldridge, A. A., MacDonald, J. A., Erdodi, F., Ma, C., Borman, M. A., Hartshorne, D. J., and Haystead, T. A. (2004) *J. Biol. Chem.* **279,** 34496–34504
21. Nakamura, K., Koga, Y., Sakai, H., Homma, K., and Ikebe, M. (2007) *Circ. Res.* **101,** 712–722
22. Neppl, R. L., Lubomirov, L. T., Momotani, K., Pfitzer, G., Eto, M., and Somlyo, A. V. (2009) *J. Biol. Chem.* **284,** 6348–6360
23. Given, A. M., Ogut, O., and Brozovich, F. V. (2007) *Am. J. Physiol. Cell Physiol.* **292,** C432–C439
24. El-Toukhy, A., Given, A. M., Ogut, O., and Brozovich, F. V. (2006) *FEBS Lett.* **580,** 5779–5784
25. Chi, A., Huttenhower, C., Geer, L. Y., Coon, J. J., Syka, J. E., Bai, D. L., Shabanowitz, J., Burke, D. J., Troyanskaya, O. G., and Hunt, D. F. (2007) *Proc. Natl. Acad. Sci. U.S.A.* **104,** 2193–2198
26. Sharma, A. K., Zhou, G. P., Kupferman, J., Surks, H. K., Christensen, E. N., Chou, J. J., Mendelsohn, M. E., and Rigby, A. C. (2008) *J. Biol. Chem.* **283,** 32860–32869
27. Lee, E., Hayes, D. B., Langsetmo, K., Sundberg, E. J., and Tao, T. C. (2007) *J. Mol. Biol.* **373,** 1198–1212
28. Choudhury, N., Khromov, A. S., Somlyo, A. P., and Somlyo, A. V. (2004) *J. Muscle Res. Cell Motil.* **25,** 657–665
29. Khromov, A. S., Wang, H., Choudhury, N., McDuffie, M., Herring, B. P., Nakamoto, R., Owens, G. K., Somlyo, A. P., and Somlyo, A. V. (2006) *Proc. Natl. Acad. Sci. U.S.A.* **103,** 2440–2445
30. Feng, J., Ito, M., Ichikawa, K., Isaka, N., Nishikawa, M., Hartshorne, D. J., and Nakano, T. (1999) *J. Biol. Chem.* **274,** 37385–37390